Hydrol. Earth Syst. Sci. Discuss., 8, 619–652, 2011
www.hydrol-earth-syst-sci-discuss.net/8/619/2011/
doi:10.5194/hessd-8-619-2011

Hydrology and Earth System Sciences Discussions

On the spatio-temporal analysis of hydrological droughts from global hydrological models

G. A. Corzo Perez[1], M. H. J. van Huijgevoort[1], F. Voß[2], and H. A. J. van Lanen[1]

[1]Hydrology and Quantitative Water Management Group, Centre for Water and Climate, Wageningen University, Droevendaalsesteeg 4, 6708 PB Wageningen, The Netherlands
[2]Center for Environmental Systems Research, University of Kassel, Kassel, Germany

Received: 23 November 2010 – Accepted: 13 December 2010 – Published: 19 January 2011

Correspondence to: G. A. Corzo Perez (corzogac@yahoo.es)

Published by Copernicus Publications on behalf of the European Geosciences Union.

Abstract

The recent concerns for world-wide extreme events related to climate change phenomena have motivated the development of large scale models that simulate the global water cycle. In this context, analyses of extremes is an important topic that requires the adaptation of methods used for river basin and regional scale models. This paper presents two methodologies that extend the tools to analyze spatio-temporal drought development and characteristics using large scale gridded time series of hydrometeorological data. The methodologies are distinguished and defined as non-contiguous and contiguous drought area analyses (i.e. NCDA and CDA). The NCDA presents time series of percentages of areas in drought at the global scale and for pre-defined regions of known hydroclimatology. The CDA is introduced as a complementary method that generates information on the spatial coherence of drought events at the global scale. Spatial drought events are found through CDA by clustering patterns (contiguous areas). In this study the global hydrological model WaterGAP was used to illustrate the methodology development. Global gridded time series (resolution 0.5°) simulated with the WaterGAP model from land points were used. The NCDA and CDA were applied to identify drought events in subsurface runoff. The percentages of area in drought calculated with both methods show complementary information on the spatial and temporal events for the last decades of the 20th century. The NCDA provides relevant information on the average number of droughts, duration and severity (deficit volume) for pre-defined regions (globe, 2 selected climate regions). Additionally, the CDA provides information on the number of spatially linked areas in drought as well as their geographic location on the globe. An explorative validation process shows that the NCDA results capture the overall spatio-temporal drought extremes over the last decades of the 20th century. Events like the El Niño Southern Oscillation (ENSO) in South America and the pan-European drought in 1976 appeared clearly in both analyses. The methodologies introduced provide an important basis for the global characterization of droughts, model inter-comparison, and spatial events validation.

HESSD

8, 619–652, 2011

1 Introduction

Drought is defined as a "sustained and regionally extensive occurrence of below average water availability" (Tallaksen and van Lanen, 2004). It is triggered by low or non rainfall, often in combination with high evaporation rates. In regions with a cold climate, deviations from normal temperatures can also give rise to drought due to early snow accumulation or late snow melt (winter drought, van Loon et al., 2010). Different types of drought can be distinguished, i.e. meteorological drought, soil moisture drought and hydrological drought (e.g., groundwater storage, river flow, lake storage) (e.g., Tallaksen and van Lanen, 2004; Wilhite, 2000; Heim Jr, 2002). Droughts have large socio-economic and environmental impacts affecting many sectors. Between 1991 and 2005, 950 million people were affected by droughts worldwide and an economic damage of 100 billion US dollar was reported (UN-IDSR, 2010). Data for Europe from 2000–2006 show that each year on average 15% of the EU total area and 17% of the EU total population have suffered from the impact of droughts. The estimated total costs of droughts for Europe over the past 30 years amounts to 100 billion Euros (EC, 2007). Climate change projections indicate continental drying and a likely associated increase in dry spell length and frequency of drought over, for instance, many mid-latitude continental interiors that will lead to significant impacts (Bates et al., 2008). There is an urgent need to adapt to the negative impacts of drought, but knowledge is still limited, in particular on how large-scale weather phenomena can be linked to hydrological drought that typically has a higher spatial variability (e.g., Fleig et al., 2010). This requires an adequate description of the spatio-temporal analysis of the different drought types, incl. how meteorological drought convert into hydrological droughts (e.g., Peters et al., 2006; Tallaksen et al., 2009) for rather large areas (e.g., region, continents or globe).

Droughts are derived preferably from observations (e.g., Lins and Slack, 1999; Douglas et al., 2000; Hisdal et al., 2001; Zhang et al., 2001; Stahl et al., 2010), but data availability is limited (e.g., Hannah et al., 2010). Combined observational-modeling frameworks are implemented for that reason. Global models that integrate

HESSD
8, 619–652, 2011

the interaction atmosphere-land (GCMs) are preferred, but their spatial scale is still too coarse to simulate sufficiently reliable land surface processes, incl. hydrological extremes. They are limited to an assessment of the average annual runoff (e.g., Milly et al., 2005). As an alternative off-line approaches have been developed over the last decades, which include Global Hydrological Models (GHMs) and Land Surface Models (LSMs) that simulate the global and continental terrestrial water cycle (e.g., Liang et al., 1994; Döll et al., 1999). The GHMs and LSMs operate at a more detailed scale than the GCMs, which allows a better representation of the hydrological processes at the land surface, which likely will lead to a better identification of hydrological extremes. These models are forced with global reanalysis meteorological datasets (e.g., Sheffield and Wood, 2008) to simulate the past water cycle or with downscaled future meteorological data derived from GCMs to generate possible future water cycles.

Recently, six LSMs and five GHMs participated in a model intercomparison project (WaterMIP) that compares simulation results of these models in a consistent way. All models were run at 0.5° spatial resolution for the global land areas for a 15 year period (1985–1999) using a newly-developed global meteorological dataset (Weedon et al., 2010b). Haddeland et al. (2010) describe the intercomparison setup and the first results of the multi-model global water balance. Most of these models also have simulated gridded time series of daily hydrological variables for the period 1958–2001 that allows inter-comparison of hydrological droughts. Methodologies have to be developed to inter-compare the spatio-temporal development of global drought among the models.

Various approaches have been proposed to describe the spatio-temporal development of drought. Peters et al. (2006) and Tallaksen et al. (2009) propose methodologies, which they apply on the river basin scale to explore the area in drought and the drought propagation in different gridded hydrometeorological variables simulated with a river basin model forced with local weather data (1960–1997). They did not consider spatially connected grid cells in drought (multi-variable, non-contiguous approach). On the continental scale Andreadis et al. (2005) studied drought in soil moisture and runoff simulated with the VIC land surface model and forced with a continental meteorological

HESSD
8, 619–652, 2011

dataset (1920–2003) to assess area in drought, but additionally to identify spatially-connected grid cells in drought and next to obtain severity-area-duration curves for the United States (multi-variable, contiguous approach, continental scale). Sheffield et al. (2009) applied the VIC model using a global meteorological forcing dataset (1950–2000) to simulate soil moisture globally. Drought characteristics (e.g., frequency, duration, severity) were derived from time series of simulated gridded data. Spatial extent of soil moisture drought was calculated for the whole globe and for 20 areas covering the world (single-variable, non-contiguous approach, global scale). Sheffield et al. (2009) also investigated spatially connected regions of soil moisture drought for each continent and globally to calculate severity-area-duration curves (single-variable, contiguous approach, global scale). Spatio-temporal analysis of drought at large scales, in particular for hydrological drought, is a relatively new concept that is still under development.

This paper aims at further development of methodologies describing the spatio-temporal development of hydrological drought (i.e. subsurface-runoff) on a global scale (non-contiguous and contiguous approaches). The methodologies are illustrated with the outcome from the global hydrological model WaterGAP (Water – Global Analysis and Prognosis, Alcamo et al., 2003) which has been widely tested in different researches (Döll and Lehner, 2002; Döll et al., 2003).

2 Spatio-temporal drought methodology

Spatial and temporal information in a drought analysis can be studied in different ways (e.g., Tallaksen et al., 2009; Hisdal et al., 2004; Hannaford et al., 2010). The particular definition of drought in this study differs from space to time, therefore an integrated drought concept is proposed. From a time series analytical point of view the definition of drought is interpreted as an anomaly of low values in the time series of the hydrological variable in a cell. On the other hand, in space a low value of a hydrological variable can be interpreted as a drought region. Therefore, the possible approaches can be represented as in Fig. 1.

HESSD
8, 619–652, 2011

– Option 1: Analysis of drought is performed by identifying anomalies determined and characterized by time series statistics (e.g., percentiles). Overall statistical information of the events are grouped and then the spatial analysis is done. A region can be built up on visual inspection of the overall information of a predefined region.

– Option 2: Analysis of drought regions in one time frame (e.g., particular day, month or year) is performed (no knowledge from past or future time frames is assumed). Regions that have the lower water flow or levels are clustered (grouped) and labelled (classified) as drought. This cluster procedure is evaluated at different time frames and matching patterns of the lower values of the regions are compared.

– Option 3: First the time dimension is considered as in Option 1, however, a second analysis is done per each time step. In evaluating the spatial regions of the drought at each time step and identifying contiguous areas it is possible to visualize the drought development.

The main objective of these three options is to cover the possible options used to develop the Non-Contiguous Drought Area (NCDA) and the Contiguous Drought Area (CDA) analyses. These two methodologies are presented here to investigate hydrological drought at large scales. The NCDA analysis in this study focuses on the globe as whole and on two selected hydroclimatic regions. Additionally, CDA analysis focuses on linked cells that have neighbours with the same conditions (e.g., drought state) and therefore can be clustered and labelled as spatial drought event.

The detailed procedure of the analysis can be divided into four steps as shown in Fig. 2. Although step 3 is not required for the CDA method it is an important analysis that helps with the overall representation of the drought region. Hereafter we present the temporal drought analysis (steps 1 and 2) followed by the NCDA and CDA methods (steps 3 and 4).

HESSD
8, 619–652, 2011

2.1 Drought analysis in the time series domain (steps 1 and 2)

To determine droughts from the modelling results the threshold level method (Yevjevich, 1967; Hisdal et al., 2004) is applied. With this method, a drought occurs when the variable of interest (e.g., precipitation, soil moisture, groundwater storage, or discharge) is below a predefined threshold (Fig. 3). The start of a drought event is indicated by the point in time when the variable falls below the threshold and the event continues until the threshold is exceeded again. Hence, each drought event can be characterised by its beginning, end and duration. Other commonly used drought characteristics are: deficit volume, calculated by summing up the differences between actual flow and the threshold level over the drought period, and minimum flow during an event (Hisdal et al., 2004; Fleig et al., 2006). Both a fixed and a variable (seasonal, monthly, or daily) threshold can be used. In this study, a monthly threshold derived from the duration curve is taken. For cells with a perennial runoff relatively low thresholds in the range from the 70 to 95-percentile can be considered reasonable (e.g., Hisdal et al., 2004). In this study the 80-percentile is selected. For cells with an intermittent or ephemeral runoff having a majority of zero flow, the 80-percentile could easily be zero in one or more months, and hence no drought events would be selected for these months. These dry regions were excluded from the drought analysis when in more than 80% of the time the simulated runoff is zero. The discrete monthly threshold values are smoothed by applying a moving average of 30 days (e.g., van Loon et al., 2010). The smoothed threshold (T) and the hydrological variable are shown in Fig. 3. To eliminate minor droughts a minimum duration of 3 days is used.

From the identification of drought events using the variable threshold method we extract the drought characteristics of each cell. The drought characteristics that fits our purpose are the average drought duration, average drought intensity and number of events. These drought characteristics are calculated as follows (similar to Sheffield et al., 2009; Tallaksen et al., 2009).

HESSD
8, 619–652, 2011

The drought duration (DD) is determined by the period of time of the variable were its value is under the drought threshold. DD^c is the total drought duration at cell c of a particular event.

$$ADD^c = \frac{\sum_{i=1}^{N^c} DD^c}{N^c} \quad (1)$$

where ADD^c is the average drought duration at cell c (N^c is the number of droughts per cell).

The deficit volume (DV) is calculated by accumulating the daily deficit ($X-T$) and visualized in Fig. 3.

$$DV_i^c = \sum_{t=t_{i_o}^c}^{t_{i_e}^c} \left(X_t^c - T_t^c\right) \quad (2)$$

where DV_i^c is the deficit volume of the event i. The initial and final time steps are represented by $t_{i_o^c}$ and $t_{i_e^c}$ respectively. T_t^c is the threshold per time step at cell c.

$$RADV^c = \frac{\sum_{i=1}^{N^c} DV_i^c}{N^c} \Big/ \mathrm{std}(X^c) \quad (3)$$

where $RADV^c$ is the relative average deficit volume at cell c. The division by the standard deviation ($\mathrm{std}(X^c)$) is required since in the following spatial analyses it is required to compare relative and not absolute values.

2.2 Spatial methodology

The two proposed methodologies, NCDA and CDA can be explained as follows.

HESSD
8, 619–652, 2011

2.2.1 Non-contiguous drought areas (NCDA, step 3)

The spatial analysis presented here is based on the occurrence of an event (binary representation). Therefore, a discrete drought state D_S^c per cell was used. This can be expressed by a function (Eq. 4).

$$D_S^c(t) = \begin{cases} 1 & \text{if} \quad X_t^c \leq T_t^c \\ 0 & \text{if} \quad X_t^c > T_t^c \end{cases} \tag{4}$$

where the drought state D_S^c per cell c at time step t is determined by the hydrological variable X at each time t.

$$\text{PDA}(t) = \sum_{c=1}^{N} (D_S^c(t) \cdot A^c)/T_{la} \cdot 100 \tag{5}$$

where PDA is the percentage of area in drought, at time t and relative to T_{la} (total land area considered, e.g., the globe, climatic region, continent). The area at each cell A^c in this study was calculated according to its projection, N is number of cells. These equations were applied to global and selected hydro-climatic regions as follows.

- Global spatial analysis of droughts
  The spatial analysis is performed by applying Eq. (5) for all cells across the globe at each time step. The result provides an overall assessment of the area in drought (% of global land area) as well as the critical periods (months or years) where this percentage is higher than normal.

- Regional drought spatial analysis (continents or climate regions)
  This approach is based on a division of the study space (globe) into regions that are defined by climate criteria. This is achieved by grouping cells that have similar climate properties. In this study we used the Köppen-Geiger classification (Köttek et al., 2006; Peel et al., 2007; Wanders et al., 2010). Wanders et al. (2010) applied

HESSD
8, 619–652, 2011

the Köppen-Geiger classification rules that define each climate to the WATCH Forcing Data (Weedon et al., 2010a) to obtain for each cell a classification. Cells that belong to the same Köppen-Geiger sub-climate were clustered. The two regions selected (Af,Cfb) in this study are highlighted in Fig. 4.

The "Af" is a tropical rainforest climate that is characterized by constant high temperatures all the year and all months have average precipitation of at least 60 mm. The clusters are mainly located in the Amazonian and Indonesian regions. The "Cfb" is a humid temperate climate, which can be generalized as climate reference for Europe, however, we know that this is relative due to the high differences in some regions in the continental and coastal regions.

2.2.2 Contiguous drought areas (CDA, step 4)

The NCDA provides the overall temporal evolution of the area in drought in a predefined region (e.g., globe, continent, hydroclimatic region). However, this pre-defined regions are arbitrary reference regions, they might separate spatially-continuous drought events (except for the case of globe as reference). Contiguous areas of drought (CDA) reflect spatial drought patterns composed by linked neighbours in a state of drought, classified here as spatial drought event. The binary representation created with the drought states (Eq. 4), from the time series analysis, allows for the application of pattern recognition techniques that group different cells based on the characteristics from their neighbours. This in general can be described as a clustering based on its neighbour conditions (e.g., connectivity). For more reference on similar type of approaches please refer to Sheffield et al. (2009) who identified drought events in time and space using other clustering algorithm, and Andreadis et al. (2005) who presented severity areas duration curves with a partitioning, smoothing and filtering process for the clustering in the spatial dimension. The method used within this study can be described as follows:

HESSD
8, 619–652, 2011

1. Scan all cells of the data first by column then by row (Fig. 5).
2. Evaluate the state of the 8 (or 4 neighbours) and assign a preliminary class (spatial drought label) to the cell. Assignation is done as follows:
   - If actual position of the cell is in drought then look for a neighbour in drought.
   - If a neighbour is in drought and has a label (class) then change the label of the actual cell to the label of the neighbour.
   - If there is more than one label between the neighbours assign the lowest one and store the equivalence in the equivalence table.
   - Else assign a new label number.
3. Resolve the table of equivalence classes leaving linked classes as one class.
4. Make a second iteration from column cells then row and relabel based on the resolved equivalence classes.

The algorithm can be applied using different numbers of neighbours, for the present study we used 8 neighbours (Dillencourt et al., 1992).

The number of spatial events is reduced applying similar criteria as other previous studies (Sheffield et al., 2009; Tallaksen et al., 2009). An areal threshold is defined with a minimum area required to have a spatial event (in this study the areal threshold was 2 cells, approx. a minimum of 5000 km^2). Therefore in this study we removed individual cells in drought from the further analysis.

3 WaterGAP model simulation

The gridded outcome from the global hydrological model WaterGAP was used in this study to further develop NCDA and CDA approaches for hydrological drought and to illustrate these across large scales. The global hydrological modeling system WaterGAP

HESSD
8, 619–652, 2011

has been widely used on exploring the distribution and availability of water resources. It has been tested against river flow data and has shown to be a powerful tool to simulate the global water cycle. WaterGAP combines a global hydrological model (Alcamo et al., 2003; Döll et al., 2003) with several global water use models (Flörke et al., 2010; Flörke and Alcamo, 2004; Alcamo et al., 2003; Döll and Siebert, 2002). The WaterGAP Global Hydrology Model calculates surface and subsurface runoff, groundwater recharge and river discharge at a spatial resolution of 0.5° and is well applicable for global assessments related to water security, food security and freshwater ecosystems. To simulate the terrestrial water cycle spatially distributed physiographic information about elevation, slope, hydrogeology, land cover and soil properties, as well as location and extend of lakes, wetlands, and reservoirs is used. In addition climate data like precipitation, temperature and different radiation terms need to be specified (see Table 1). Optionally, water required for consumptive water use can be subtracted from surface waters. In this study only naturalized model simulations (i.e. without taking water management and water uses into account) were utilized. As a hydrological variable the simulated daily, gridded sub-surface runoff was used. For the spatio-temporal analysis presented in this study the WaterGAP model has been set-up with the characteristics presented in Table 1. We used the WATCH forcing data (Weedon et al., 2010a,b) to force the WaterGAP model. The WATCH forcing variables are taken from the ERA-40 reanalysis product of the European Centre for Medium Range Weather Forecasting (ECMWF) as described by Uppala et al. (2005), and are interpolated to 0.5° spatial resolution, including elevation corrections as well as different methods for bias and/or undercatch corrections. For detailed information on the forcing variables see Weedon et al. (2010a,b). The spatial resolution of the forcing and model results for each hydrological variable is 0.5° latitude by longitude, covering land areas defined by the CRU (Climate research unit of the University of East Anglia) land mask.

HESSD
8, 619–652, 2011

4 Results

The study of the CDA and NCDA was evaluated for two different time periods. A long record of 38 years starting in 1963 was used for the NCDA. Part of this record, starting from 1976 (25 years) was used for the CDA. The period for the CDA was selected based on the highest number of droughts found in the run of the NCDA analysis. In addition to this the CDA computational time is higher and therefore this shorter period was beneficial. Both for the NCDA and the CDA, the same variable threshold was used for each cell, which was derived from the time series that cover the whole period of 38 years. Only land point cells from the CRU mask were considered in this analysis (total land area is 146 698 277 km^2; distributed over 67 420 cells).

4.1 Time series results

Figure 6a–c shows global maps with the different drought characteristics. Some regions are classified as dry climates when threshold equals zero (in more than 80% of time no calculated runoff from grid cell). One would expect a clear negative correlation between N^c and the ADD^c. The different characteristics do not show high visual pattern similarities. For instance, the number of events (N^c) shows a high number in the Amazonian river basin. In contrast, the ADD^c is high in the northern part of Africa. This can be explained by the prolonged duration of low flows in that part of Africa. The distribution of the relative average deficit volume (RADV^c) is mixed and only spotted values can be seen without a clear region or predominance. Figure 6d shows the drought pattern at the beginning of 1963. The drought characteristics presented in Fig. 6 show the importance of exploring the NCDA and CDA techniques presented in the following. The NCDA global results can be visualized at each time step (Fig. 6d) or as part of an analysis of the global drought characteristics (Fig. 6a–c). The global drought characteristics show visual discrepancy between one time step (Fig. 6d) and the overall analysis (Fig. 6a–c). This is expected since the statistical mean of the different values might not represent well the dynamics of the droughts. In this case we can see concentration of

HESSD
8, 619–652, 2011

high numbers of droughts in the Amazonia river basin (South America) and in some other river basins in Africa and Asia (Fig. 6d), in contrast to the other three graphs.

4.2 Global results (NCDA)

The Percentage of Drought Area (PDA) for each time step are explored using Eq. (5). Figure 7a shows the evolution of the PDA of the whole globe for the period between 1963 till 2000. From the yearly time series it is possible to derive the bound of maximum and minimum PDA, 30% and 12% respectively. The maximum PDA appears at the time series for the year 1992.

The color-coded map in Fig. 7b is built using the time series of PDA and a color representation for each percentage. The color-coded table shows some persistence among the years. It shows the onset and end of multiple years in droughts. Furthermore, Fig. 7b shows a low percentage of area in drought between the beginning of 1974 to the middle of the year 1976, as well as from the beginning of 1978 to first months of 1980. On the other hand, higher percentages can be seen from April till July 1982 and from February till August 1992. The highest percentage in 1992, seems to be not clearly preceded by other dry years. Other high PDAs can be seen in 1997 where the beginning of the high percentage appears at the end of 1996. Most of the historical high PDA are located between calendar day 100 to 150 (April–May). This might seem to happen on the early summer for the Northern Hemisphere and transition summer–autumn in the Southern Hemisphere. The last 130 days of the time series seems to stable and no important variations can be seen from the beginning (day 230) to the end (360) of most of the years.

4.3 Köppen-Geiger hydro-climatic regions (NCDA)

Percentages of drought areas also were calculated for 2 hydroclimatic regions to investigate the spatial differences in the areal coverage across the world.

HESSD
8, 619–652, 2011

Figure 8a shows the 38 annual series of the PDA for the clusters with a Af climate. The PDA values are higher than in the overall analysis for the globe (Fig. 7a), reaching a value of 62% at the beginning of 1997 and the end of 1998. This is a region that is well known for its richness in water resources on average, nevertheless, it appears to have a high number of anomalies in its low runoff, which can be explained by the rather large inter annual variability. Aside of this, in the year 1992 the most severe PDA over a whole year is shown.

For the second climate regime (Cfb, Fig. 4), the highest PDA is 36% (Fig. 8b). In this hydroclimatic region, 1992 seems not to have a high area in drought. The year 1976 has the highest PDA for the Cfb region. In the discussion section, the above-mentioned years with high PDAs will be compared with some events documented in the literature.

4.4 Spatial drought events (CDA)

In contrast to the NCDA presented in the previous sections, the contiguous approach (CDA) presented here focuses on linking neighbouring drought states. Therefore, connected D_S^c can be interpreted as a spatial drought event, which is a cluster of cells. Each spatial event, which is unique for a particular time step, can be analysed further by exploring its spatial properties. Figure 9(a) shows the results of a clustering analysis for the 10 January 1967. For this date more than 800 spatial drought events were found. To explore the temporal evolution of the number of spatial drought events a color-coded table of 27 years with the number of clusters found on each day was plotted (Fig. 9(b)). The figure shows similar patterns as the NCDA. Only less than 300 spatial drought events did not appear. The year 1992 stands out as in the NCDA as the most critical year. Other extreme events, like 1982, 1987, 1992 and 1993 also show up in this graphical presentation. This illustrates that the number of spatial drought events seems to be consequent with the global area in drought.

Figure 9(a) illustrates that the distribution of the spatial drought events does not follow hydroclimatic classifications. Spatial drought events do not follow clear climatic

HESSD
8, 619–652, 2011

or regional (e.g., continents) boundaries and its areas can be in multiple hydroclimatic regions at the same time. Boundaries of climate regions may separate spatial events.

The main advantages of the CDA are the possibilities to specify: (i) the area of a particular spatial event (number of cells or area), and (ii) location (geo-referenced). This can be done for a specific time step as demonstrated in Fig. 9a. Additionally, in a temporal study it also requires monitoring the evolution of spatial drought events for a (long) time series (e.g., Andreadis et al., 2005), as well as to summarize statistically their information. In this study we monitor the time (i.e. number of days) that the maximum area of a spatial drought event occurs somewhere in the world. This was done to keep track of the change in a Maximum Spatial Drought Events (MSDE, labelled clusters) in terms of it relative location at each time step. Figure 10a shows a color-coded table with the timing and the magnitude of the MSDE for each day within the 25 year record contemplated in this part of the study. MSDE of above 5000 cells (about 7.5% of the global land area) appear only around 6 times for a maximum of 30 days.

To explore the number of occurrence of the maximum spatial drought event in a continent we identified the number of days that the centroid of the global maximum event was found in that continent. Figure 10(b) shows how many days the centroid of the maximum global spatial drought event occurs in the different continents. For instance, in 1999 the maximum event was found in Asia for over 300 days and for about 50 days in North America. The maximum area seems to be located predominantly in Asia. Africa has continuous record with events from 1983 till 1985. Exceptional cases in Europe can be highlighted like 1976 which has a high number of days with the maximum spatial drought event (over 60 days).

5 Discussion

An unique formulation is required for the characterization of spatial drought events, since conventional averaging of spatial regions might not really represent relevant characteristics of the drought. The duration of a spatial event could be defined by the

HESSD
8, 619–652, 2011

average, longest or shortest duration of the cluster of connected neighbourhood cells. However, to determine a deficit volume that is part of a particular spatial event it might not be accurate to add directly deficits. Instead, a weighting of normalized volumes can be calculated as an alternative. Lastly, the spatial extent of the events is changing in time, as well as its centroid, therefore a morphological and dynamic analysis needs to be included in the CDA method presented in this paper. In this sense, this paper did not cover the drought characteristics of these spatial events (e.g. representative drought duration or deficit volume of a cluster).

Aside of this the validation of some of the results was done by looking at historical events in the world. In general, the NCDA and CDA results agree with major historical events. The years 1997 and 1998, which correspond to the ENSO phenomena (clearly present in Indonesia and South America, Aceituno, 1988; Chokkalingam et al., 2005), show to have a clear high percentage of drought area in the NCDA (Af region) and clearly a high number of spatial drought events can be found in the CDA.

The European drought in 1976 is clearly elucidated in the CDA and NCDA, and its durations seem to match with previous studies (Hisdal et al., 2004; Hannaford et al., 2010). The Cfb region has an important component in Europe (Fig. 8(b)) and in many studies the 1976 European drought has been studied due to the high economical losses for many countries (Stahl, 2001). Although in our study, with the CDA, the maximum spatial event in 1976 is not as high as it was expected (Fig. 8a), that year had a long period of time with the maximum drought event in the globe. Also in 1991/1992 there was a prolonged drought over the Iberia peninsula (Hisdal et al., 2004). The United States experienced severe to extreme drought in over half of the country during 1987–1989. This drought was the subject of national headlines when it resulted in the extensive fires in Yellowstone National Park in 1988 (Sheffield et al., 2009; Andreadis et al., 2005; Shukla and Wood, 2008). It is documented that Africa suffered from droughts in the last quarter of the twentieth century (Prospero and Nees, 1986). Ethiopia, usually considered the breadbasket of Eastern Africa, was hit by a brutal drought in the early 1980's. A dry year in 1981 resulted in low crop yields.

HESSD
8, 619–652, 2011

By applying the NCDA with hydroclimatic regions that are affected by events like the El niño southern oscillation (ENSO) can be useful to validate the model, since in the overall information it is not possible to capture this phenomena. Other regional distributions of the earth, can help on model inter-comparison, since models might perform better or worst according to different hydroclimatic regions.

6 Conclusions

In this study, two concepts of spatio-temporal analysis of large-scale drought have been further developed. These concepts are the non-contiguous drought areas (NCDA) and the contiguous drought areas (CDA) approach. The NCDA analysis over the globe and pre-defined hydroclimatic regions followed the principles used at the river basin scale proposed by Tallaksen et al. (2009). In a similar way, temporal analysis with a variable threshold followed by spatial assessment was presented. The CDA presented here builds on the use of an objective and automatic grouping of spatial drought events. This objective determination of spatial drought events is based on pattern recognition using binary images and connected labeling algorithms. The NCDA and CDA analyses were performed over the subsurface flow values from the WaterGAP global hydrological model (second part 20th century).

The NCDA is useful on assessing overall spatial drought information at global and regional scales (i.e. climate regions), while the CDA shows large spatially-connected drought events that are unbounded by predefined regions, and clearly cut through these as defined in the NCDA. The analyses also illustrates that there is a positive correlation between the global area in drought (NCDA) and the number of spatial drought events (CDA).

The NCDA was useful on assessing overall spatial drought information at global and regional scales, while CDA showed specific extreme areas clearly and unbound by predefined regions. NCDA results seem to capture important events that might appear to be connected to relevant historical events. The ENSO phenomena and the droughts

HESSD
8, 619–652, 2011

in Europe (1976 and 1993) were present in different ways in both methods. With the NCDA a high percentage of area was identified and with the CDA a high area spatial event was found.

The centroid of the maximum spatial drought event in the CDA analysis was used as reference of extreme events in the different continents. Its duration is assumed to be determined by the persistence of the maximum event in a continent. It appears that there is a season where drought event tend to occur (April–May). Information about large area events was found and results show that they seem to occur on long periods in different continents. Validation of this information was discussed showing agreement with historical information. Especially with the maximum spatial drought in 1976 which appeared to be related with the historical event.

The CDA shows to be able to have a more objective identification of spatial drought events and at the same time it is possible to follow critical (the most extended) events along time in many continents. However, important variables like volume and duration do require an analysis to be able to reach indexes that characterize their drought degree. Aside of this, morphological changes and tracking of spatial drought events seems to be the way forward to explore more the spatial events and see how well models capture historical events. Although the CDA methodology presented here is used on subsurface flow, it is possible to apply the same procedures for similar variables and other drought identification approaches, e.g. the Sequent Peak Algorithm (Hisdal et al., 2004). Further research steps are being taken towards the sensitivity of the thresholds in the drought identification of spatial events, tracking of spatial drought events and multi-model comparisons.

Acknowledgement. This research was undertaken as part of the European Union (FP6) funded Integrated Project Water and Global Change (WATCH, contract 036946). The research is part of the programme of the Wageningen Institute for Environment and Climate Research (WIMEK-SENSE).

HESSD
8, 619–652, 2011

References

Aceituno, P.: On the functioning of the Southern Oscillation in the South American sector, Part I: Surf. climate, Mon. Weather Rev., 116, 505–524, 1988. 635

Alcamo, J., Döll, P., Henrichs, T., Kaspar, F., Lehner, B., Rösch, T., and Siebert, S.: Development and testing of the WaterGAP 2 global model of water use and availability/Développement et évaluation du modèle global WaterGAP 2 d'utilisation et de disponibilité de l'eau, Hydrolog. Sci. J., 48, 317–337, 2003. 623, 630

Andreadis, K., Clark, E., Wood, A., Hamlet, A., and Lettenmaier, D.: Twentieth-century drought in the conterminous United States, J. Hydrometeorol., 6, 985–1001, 2005. 622, 628, 634, 635

Bates, B., Kundzewicz, Z., Wu, S., and Palutikof, J.: Climate Change and Water: Technical Paper of the Intergovernmental Panel on Climate Change, Intergovernmental Panel on Climate Change, 2008. 621

Batjes, N.: A world dataset of derived soil properties by FAO–UNESCO soil unit for global modelling, Soil Use Manage., 13, 9–16, 1997. 642

Chokkalingam, U., Kurniawan, I., and Ruchiat, Y.: Fire, livelihoods, and environmental change in the middle Mahakam peatlands, East Kalimantan, Ecol. Soc., 10, 26, 2005. 635

Dillencourt, M. B., Samet, H., and Tamminen, M.: A general approach to connected-component labeling for arbitrary image representations, J. ACM, 39, 253–280, doi:10.1145/128749.128750, 1992. 629

Döll, P. and Lehner, B.: Validation of a new global 30-min drainage direction map, J. Hydrol., 258, 214–231, 2002. 623, 642

Döll, P. and Siebert, S.: Global modeling of irrigation water requirements, Water Resour. Res., 38(4), 8.1–8.10, doi10.1029/2001WRR000355, 2002. 630

Döll, P., Kaspar, F., and Alcamo, J.: Computation of global water availability and water use at the scale of large drainage basins, Math. Geol., 4, 111–118, 1999. 622

Döll, P., Kaspar, F., and Lehner, B.: A global hydrological model for deriving water availability indicators: model tuning and validation, J. Hydrolog., 270, 105–134, 2003. 623, 630

Douglas, E., Vogel, R., and Kroll, C.: Trends in floods and low flows in the United States: impact of spatial correlation, J. Hydrol., 240, 90–105, 2000. 621

EC: Communication Addressing the challenge of water scarcity and droughts in the European Union, http://ec.europa.eu/environment/water/quantity/scarcity_en.htm, last access: 30

HESSD
8, 619–652, 2011

September 2010, European Commission, COM (2007), 414 final, Brussels, 2007. 621
Fleig, A. K., Tallaksen, L. M., Hisdal, H., and Demuth, S.: A global evaluation of streamflow drought characteristics, Hydrol. Earth Syst. Sci., 10, 535–552, doi:10.5194/hess-10-535-2006, 2006
Fleig, A. K., Tallaksen, L. M., Hisdal, H., and Hannah, D. M.: Regional hydrological drought in north-western Europe: linking a new Regional Drought Area Index with weather types, Hydrol. Process., doi:10.1002/hyp.7644, 2010. 621
Flörke, M. and Alcamo, J.: European outlook on water use, Center for Environmental Systems Research, University of Kassel, Final Report, EEA/RNC/03/007, 2004. 630
Flörke, M., Bärlund, I., and Teichert, E.: Future changes of freshwater needs in European power plants, Management of Environmental Quality, doi:10.1108/14777831111098507, 2010. 630
Haddeland, I., Clark, D., Franssen, W., Ludwig, F., Voss, F., Arnell, N., Bertrand, N., Best, M., Folwell, S., Gerten, D., Gomes, S., Gosling, S. N., Hagemann, S., Hanasaki, N., Harding, R., Heinke, J., Kabat, P., Koirala, S., Oki, T., Polcher, J., Stacke, T., Viterbo, P., Weedon, G. P., and Yeh, P.: Multi-model estimate of the global water balance: setup and first results, J. Hydrometeor., under review, 2010. 622
Hannaford, J., Lloyd-Hughes, B., Keef, C., Parry, S., and Prudhomme, C.: Examining the large-scale spatial coherence of European drought using regional indicators of precipitation and streamflow deficit, Hydrol. Process., doi:10.1002/hyp.7725, 2010. 623, 635
Hannah, D. M., Demuth, S., van Lanen, H. A. J., Looser, U., Prudhomme, C., Rees, R., Stahl, K., and Tallaksen, L. M.: Large-scale river flow archives: importance, current status and future needs, Hydrol. Process., doi:10.1002/hyp.7794, 2010. 621
Heim Jr., R.: A review of twentieth-century drought indices used in the United States, B. Am. Meteorol. Soc., 83, 1149–1165, 2002. 621
Hisdal, H., Stahl, K., Tallaksen, L. M., and Demuth, S.: Have streamflow droughts in Europe become more severe or frequent?, Int. J. Climatol., 21, 317–333, 2001. 621
Hisdal, H., Tallaksen, L., Clausen, B., Peters, E., and Gustard, A.: Hydrological drought characteristics, Hydrological drought, Processes and estimation methods for streamflow and groundwater, in: Developments in Water Science, 48, Elsevier Science B.V., 139–198, 2004 623, 625, 635
Köttek, M., Grieser, J., Beck, C., Rudolf, B., and Rubel, F.: World map of the Köppen-Geiger climate classification updated, Meteorol. Z., 15, 259–263, 2006. 627
Lehner, B. and Döll, P.: Development and validation of a global database of lakes, reservoirs

HESSD
8, 619–652, 2011

and wetlands, J. Hydrol., 296, 1–22, 2004. 642
Liang, X., Lettenmaier, D., Wood, E., and Burges, S.: A simple hydrologically based model of land surface water and energy fluxes for general circulation models, J. Geophys. Res., 99, 14415–14428, 1994. 622
Lins, H. and Slack, J.: Streamflow trends in the United States, Geophys. Res. Lett., 26, 227–230, 1999. 621
Loveland, T., Reed, B., Brown, J., Ohlen, D., Zhu, Z., Yang, L., and Merchant, J.: Development of a global land cover characteristics database and IGBP DISCover from 1 km AVHRR data, Int. J. Remote Sens., 21, 1303–1330, 2000. 642
Milly, P., Dunne, K., and Vecchia, A.: Global pattern of trends in streamflow and water availability in a changing climate, Nature, 438, 347–350, 2005. 622
Peel, M. C., Finlayson, B. L., and McMahon, T. A.: Updated world map of the Köppen-Geiger climate classification, Hydrol. Earth Syst. Sci., 11, 1633–1644, doi:10.5194/hess-11-1633-2007, 2007. 627
Peters, E., Bier, G., van Lanen, H. A. J., and Torfs, P. J. J. F.: Propagation and spatial distribution of drought in a groundwater catchment, J. Hydrol., 321, 257–275, 2006. 621, 622
Prospero, J. and Nees, R.: Impact of the North African drought and El Nino on mineral dust in the Barbados trade winds, Nature, 320, 735–738, 1986. 635
Sheffield, J. and Wood, E.: Global trends and variability in soil moisture and drought characteristics, 1950–2000, from observation-driven simulations of the terrestrial hydrologic cycle, J. Climate, 21, 432–458, 2008. 622
Sheffield, J., Andreadis, K., Wood, E., and Lettenmaier, D.: Global and continental drought in the second half of the twentieth century: Severity-area-duration analysis and temporal variability of large-scale events, J. Climate, 22, 1962–1981, 2009. 623, 625, 628, 635
Shukla, S. and Wood, A.: Use of a standardized runoff index for characterizing hydrologic drought, Geophys. Res. Lett., 35, L02405, doi:10.1029/2007GL032487, 2008. 635
Stahl, K.: PhD thesis: Hydrological drought – a study across Europe, Ph.D. thesis, Universitätsbibliothek Freiburg, Germany, 2001. 635
Stahl, K., Hisdal, H., Hannaford, J., Tallaksen, L. M., van Lanen, H. A. J., Sauquet, E., Demuth, S., Fendekova, M., and Jódar, J.: Streamflow trends in Europe: evidence from a dataset of near-natural catchments, Hydrol. Earth Syst. Sci., 14, 2367–2382, doi:10.5194/hess-14-2367-2010, 2010. 621
Tallaksen, L. M. and van Lanen, H. A. J.: Hydrological drought: processes and estimation meth-

HESSD
8, 619–652, 2011

ods for streamflow and groundwater, Developments in Water Science, 48, Elsevier Science B.V., 2004. 621

Tallaksen, L. M., Hisdal, H., and van Lanen, H. A. J.: Space-time modelling of catchment scale drought characteristics, J. Hydrol., 375, 363–372, 2009. 621, 622, 623, 625, 636

Uppala, S., Kallberg, P., Simmons, A., Andrae, U., Bechtold, V., Fiorino, M., Gibson, J., Haseler, J., Hernandez, A., Kelly, G. A., Li, X., Onogi, K., Saarinen, S., Sokka, N., Allan, R. P., Andersson, E., Arpe, K., Balmaseda, M. A., Beljaars, A. C. M., Van De Berg, L., Bidlot, J., Bormann, N., Caires, S., Chevallier, F., Dethof, A., Dragosavac, M., Fisher, M., Fuentes, M., Hagemann, S., Holm, E., Hoskins, B. J., Isaksen, L., Janssen, P., Jenne, R., Mcnally, A. P., Mahfouf, J. F., Morcrette, J. J., Rayner, N. A., Saunders, R. W., Simon, P., Sterl, A., Trenberth, K. E., Untch, A., Vasiljevic, D., Viterbo, P., and Woollen, J.: The ERA-40 re-analysis, Quarterly Journal of the Royal Meteorological Society, 131, 2961–3012, 2005. 630

van Loon, A. F., van Lanen, H. A. J., Hisdal H., Tallaksen L.M., Fendeková, M., Oosterwijk, J., Horvát, O., and Machlica: A. Understanding hydrological winter drought in Europe, in: Global Change: Facing Risks and Threats to Water Resources, IAHS Publ. No. 340, 189–197, 2010. 621, 625

Wanders, N., van Lanen, H. A. J., and van Loon, A. F.: Indicators for drought characterization on a global scale. WATCH Technical Report no. 24, available at: http://www.eu-watch.org/nl/25222760-Technical_Reports.html, last access: 22 November 2010, 2010. 627

Weedon, G., Gomes, S., Viterbo, P., Shuttleworth, J., Blyth, E., Sterle, H., Adam, J., Bellouin, N., Boucher, O., and Best, M.: Evidence of changing evaporation in the late twentieth century from the WATCH Forcing Dataset, J. Hydrometeorol., submitted, 2010a. 630

Weedon, G. P., Gomes, S., Viterbo, P., Österle, H., Adam, J. C., Bellouin, N., Boucher, O., and Best, M.: The WATCH Forcing Data 1958–2001: a meteorological forcing dataset for land surface- and hydrological-models., Tech. rep., WATCH Technical Report no. 22, available at: http://www.eu-watch.org/nl/25222760-Technical_Reports.html, last access: 30 September 2010, 2010b. 622, 630

Wilhite, D.: Drought: a global assessment, Routledge, London, New York, 2000. 621

Yevjevich, V.: Objective Approach to Definitions and Investigations of Continental Hydrologic Droughts, Hydrology Paper 23, Colorado State U, Fort Collins, August 1967, 19 p., 9 fig., 1 tab., 12 ref., 1967. 625

Zhang, X., Harvey, K., Hogg, W., and Yuzyk, T.: Trends in Canadian streamflow, Water Resour. Res., 37, 987–998, 2001. 621

HESSD

8, 619–652, 2011

Table 1. WaterGAP model setup information.

Forcing	Veg balance	Soil data	Soil information used	Lakes/ wetlands	Routing network
precipitation, temperature, shortwave down (incoming shortwave) and net longwave radiation	global land cover characterization (Loveland et al., 2000, GLCC, IGBP)	world dataset of derived soil properties (Batjes, 1997, FAO)	land cover type dependent field capacity; permafrost included in gw-factor	GLWD (Lehner and Döll, 2004)	DDM30 (Döll and Lehner, 2002)

HESSD
8, 619–652, 2011

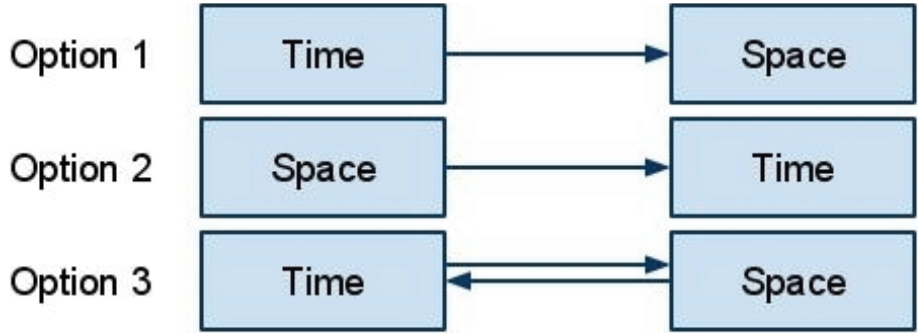

Fig. 1. Diagram of the steps in a temporal and spatial analysis.

HESSD
8, 619–652, 2011

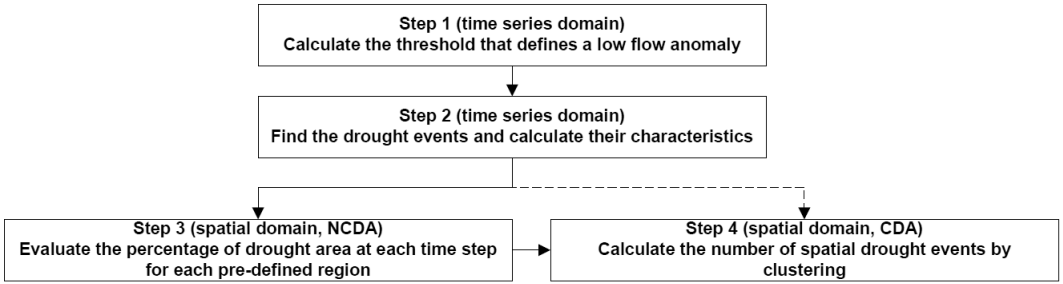

Fig. 2. Diagram of temporal and spatial analysis interaction.

HESSD
8, 619–652, 2011

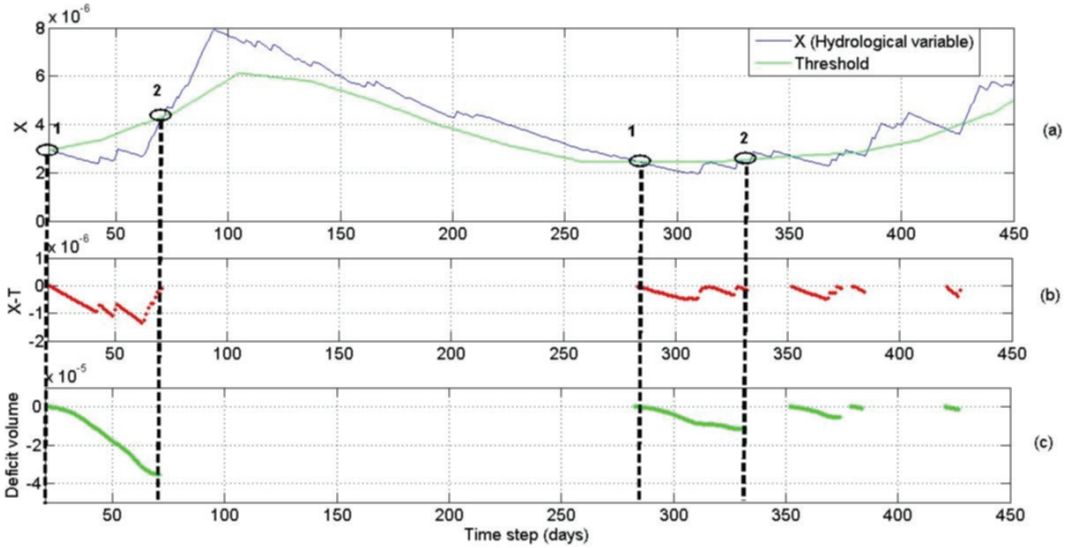

Fig. 3. Drought characteristics calculated with variable threshold: **(a)** Hydrological variable and variable threshold, **(b)** daily intensity, **(c)** event deficit volume. Start and end of the events are named as 1 and 2.

HESSD
8, 619–652, 2011

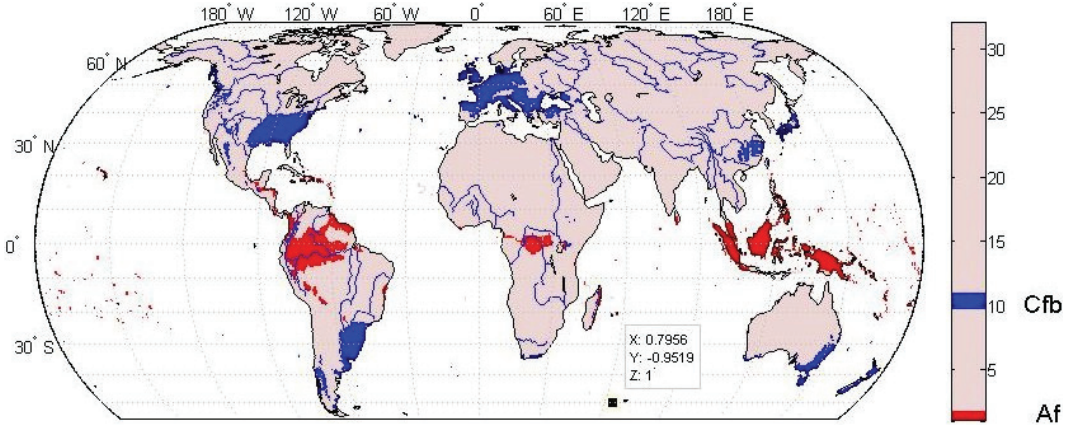

Fig. 4. Distribution of clusters for selected cells with the Köppen-Geiger Af (red) and Cfb (blue) sub-climates around the world using the WATCH Forcing Data.

HESSD
8, 619–652, 2011

0	1	0	0	0
1	1	0	0	0
0	0	1	0	1
0	1	0	0	1

0	C1	0	0	0
C1	C1	0	0	0
0	0	C1	0	C3
0	C2	0	0	C3

(a) Step 1

Equivalences	
1	1,2
2	1,2
3	3

0	C1	0	0	0
C1	C1	0	0	0
0	0	C1	0	C3
0	C1	0	0	C3

(b) Step 2

Fig. 5. Example of the steps for linking neighbours in a drought cluster (for detailed explanations see text).

HESSD
8, 619–652, 2011

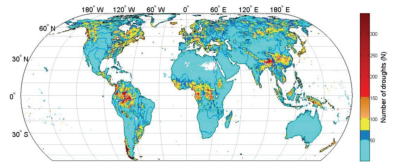

(a) Total number of drought events

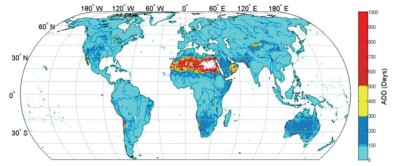

(b) Average drought duration

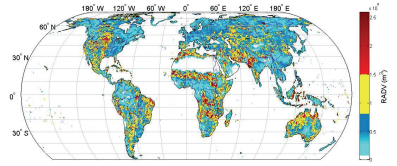

(c) Relative average deficit volume

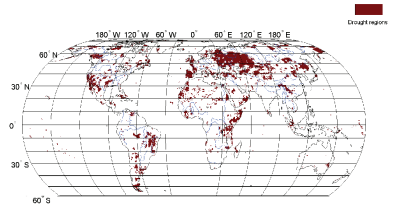

(d) Spatial distribution of drought events for 13 January 1976

Fig. 6. Hydrological drought characteristics derived from the sub-surface runoff simulated with the WaterGAP model.

HESSD
8, 619–652, 2011

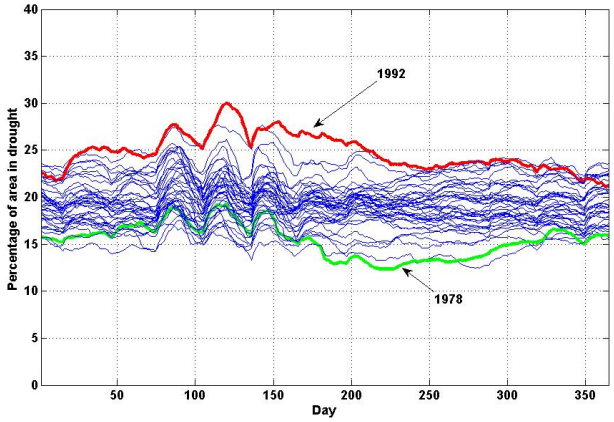

(a) Time series of area in drought (percentage of the globe) for the period 1963–2000

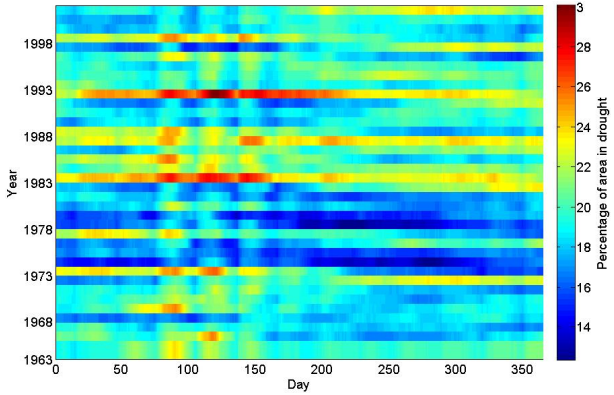

(b) Color-coded table of area in drought (percentage of the globe) for the period 1963–2000

Fig. 7. Hydrological drought derived from the sub-surface runoff simulated with the WaterGAP global hydrological model.

HESSD
8, 619–652, 2011

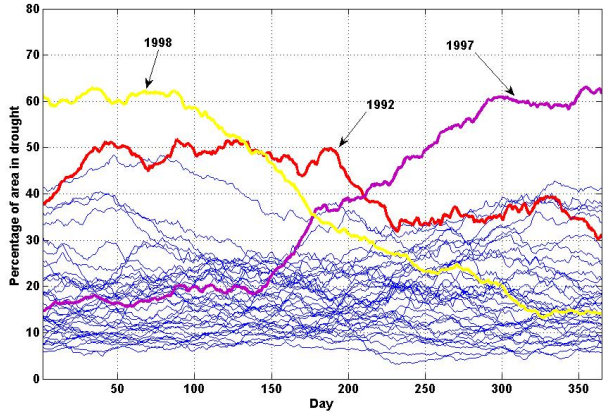

(a) Areas with tropical rainforest climate (Af)

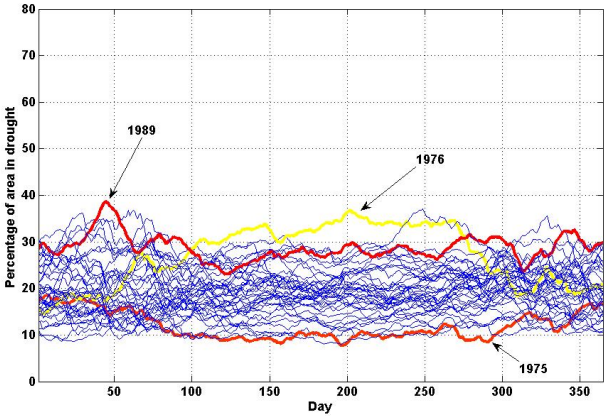

(b) Areas with maritime, temperate climate (Cfb)

Fig. 8. Daily time series of percentage of area in drought for each year in the period 1963 to 2001 in Af and Cfb climates.

HESSD
8, 619–652, 2011

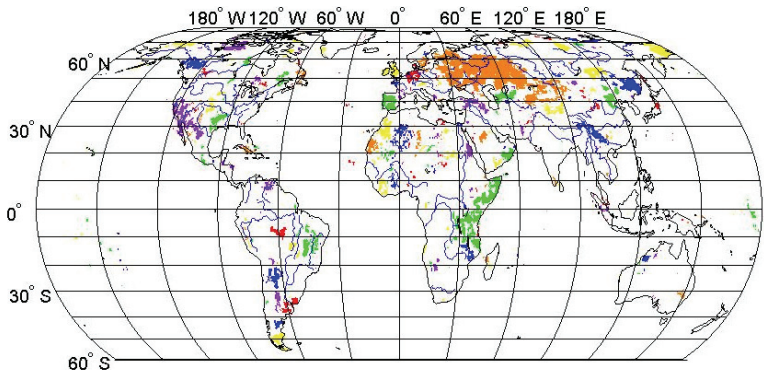

(a) Drought clusters for the 10th of January 1976

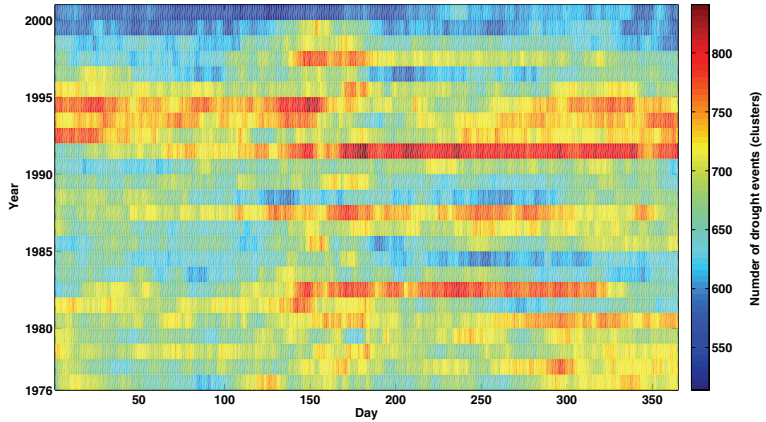

(b) Color-coded table of the number of drought clusters on the whole Earth

Fig. 9. Results of the CDA method applied for the analysis of number of drought clusters.

HESSD
8, 619–652, 2011

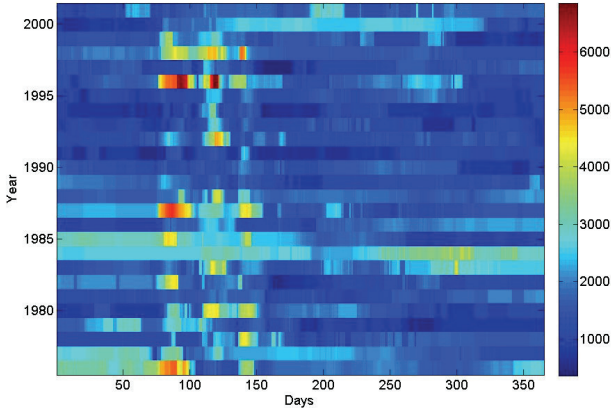

(a) Maximum area of the spatial drought event (in cells) for the period 1976–2000

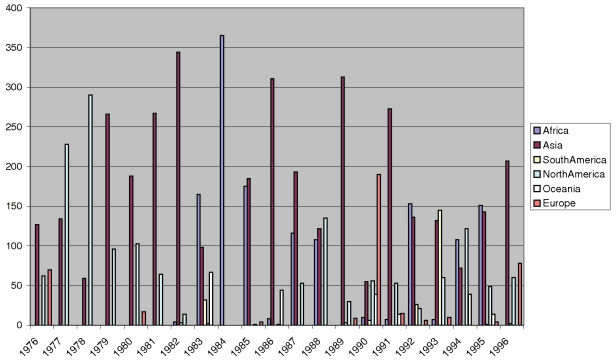

(b) Location of the maximum spatial drought event and number of days

Fig. 10. Occurrence and duration of the maximum spatial drought events for the period 1976–2000.

HESSD
8, 619–652, 2011